Appl Compos Mater (2018) 25:527–544
DOI 10.1007/s10443-017-9633-5

Process Modelling of Curing Process-Induced Internal Stress and Deformation of Composite Laminate Structure with Elastic and Viscoelastic Models

Dongna Li[1] **· Xudong Li**[1] **· Jianfeng Dai**[2]

Received: 15 July 2017 / Accepted: 28 July 2017 / Published online: 10 August 2017

Abstract In this paper, two kinds of transient models, the viscoelastic model and the linear elastic model, are established to analyze the curing deformation of the thermosetting resin composites, and are calculated by COMSOL Multiphysics software. The two models consider the complicated coupling between physical and chemical changes during curing process of the composites and the time-variant characteristic of material performance parameters. Subsequently, the two proposed models are implemented respectively in a three-dimensional composite laminate structure, and a simple and convenient method of local coordinate system is used to calculate the development of residual stresses, curing shrinkage and curing deformation for the composite laminate. Researches show that the temperature, degree of curing (DOC) and residual stresses during curing process are consistent with the study in literature, so the curing shrinkage and curing deformation obtained on these basis have a certain referential value. Compared the differences between the two numerical results, it indicates that the residual stress and deformation calculated by the viscoelastic model are more close to the reference value than the linear elastic model.

Keywords Three-dimensional finite element analysis · Thermosetting composite · Residual stress · Curing Shrinkage · Deformation

1 Introduction

The thermosetting resin composites are widely used in the field of aerospace with its high specific strength, high specific stiffness and other excellent mechanical properties. However,

✉ Dongna Li
lidongna9895@163.com

[1] School of Materials Science and Engineering, Lanzhou University of Technology, Lanzhou 730050, China

[2] School of Science, Lanzhou University of Technology, Lanzhou 730050, China

during the curing process of composite materials, several phenomena, such as inherent anisotropy, thermal expansion, chemical shrinkage and materials degradation or relaxation, can lead to the generation and development of residual stress and deformation of the composite structures [1–3]. Thus, it is imperative to reduce the residual stress and control the curing deformation in improving the quality of composites forming and reducing costs. The traditional method of compensating the mold surface is time consuming and laborious. Adopting computer finite element analysis technology can effectively analyze and predict the curing process of composites.

In recent years, many scholars have used finite element analysis method to simulate the curing deformation of composite materials [4–12], and different models have been presented to predict the stress and deformation due to non-uniform temperature and DOC [13–20]. Owe to suitable constitutive models including aforementioned factors, the stress and deformation of the composite structures can effectively describe the mechanical response evolution during cure cycle. Among them, elastic model and viscoelastic model are the common metods to predict the residual stress development for the composites. It is generally known that the polymer shows viscoelastic properties during cure cycle, especially at heat-up cycle and hold cycle. Linear elastic model can only be used to predict the internal stress developing at cool-down cycle, and the stress development during curing is neglected [21, 22]. It cannot describe the viscoelastic behavior of the composites during curing. Therefore, some other researchers prefer viscoelastic constitutive model to describe the viscoelastic characteristic for the composite materials during cure cycle [23, 24]. Because the curing of composite materials is a multi-physics coupling problem about temperature, DOC and stress field, combining these constitutive models with FEA, the internal stress and deformation of the composite laminates during whole cure process can be predicted effectively and accurately [25]. Although viscoelastic model has obvious advantage in increasing accuracy, the scarcity of experimental evidence, long runtimes and difficult numerical implementation are the stumbling blocks for its extensive application [26]. Therefore, the linear elastic model is sometimes a better choice in the case of low accuracy standard.

In this paper, both the linear elastic model and the viscoelastic model are employed in a three-dimensional composite laminate structure with the performance parameters of the AS4/3501-6 carbon fiber epoxy resin to calculate process-induced residual stress and deformation during cure cycle of the composite laminates. Then, the simulation results from two different models are compared with each other, and the existing simulation results in literature are used as references. Finally, the suitable model can be selected on the basis of practical conditions and requirements according to the comparative result.

2 Theoretical Model and Relevant Material Parameters

2.1 Heat Conduction Equation

The heat of the composite material is mainly derived into two aspects. First, the external heat of the composite material is transferred to the composite material structure, and the other part is the nonlinear heat source produced by the chemical reaction of the matrix resin curing process. In this paper, we use Fourier heat conduction law and energy balance to establish mathematical model [1, 2]. The three-dimensional transient heat conduction control equation is:

$$\rho_c C_{pc} \frac{\partial T}{\partial t} = \frac{\partial}{\partial x}\left(k_x \frac{\partial T}{\partial x}\right) + \frac{\partial}{\partial y}\left(k_y \frac{\partial T}{\partial y}\right) + \frac{\partial}{\partial z}\left(k_z \frac{\partial T}{\partial z}\right) + \frac{\partial Q}{\partial t} \tag{1}$$

where ρ_c and C_{pc} are the density and the specific heat capacity of the composites, respectively; k_x, k_y and k_z are the anisotropic thermal conductivities of the composites in the x, y and z directions; t is the absolute time; T is the transient temperature of the composites at time t, and Q is the internal heat source, which can be expressed by the following equation:

$$\frac{\partial Q}{\partial t} = \rho_r (1 - v_f) H_R \frac{d\alpha}{dt} \tag{2}$$

where ρ_r is the density of the resin matrix; v_f is the fiber volume fraction of the composites; α and $d\alpha/dt$ are the DOC and the curing rate of the resin matrix, respectively, and H_R is the total release heat during curing.

During the curing process, the thermo-physical properties of the composites and their constituents, including density, specific heat capacity and thermal conductivity vary with temperature and DOC. The thermo-physical properties of AS4 carbon fiber and 3501-6 epoxy resin are shown in Table 1, and the thermo-physical properties of the composites can be calculated by the rule of mixtures (15)-(18) presented in Appendix.

2.2 Cure Kinetics Model

The curing reaction of the resin matrix is a heat-activated complex chemical cross-linking reaction, so most of the equations related to the kinetics of the curing reaction are based on the empirical model. In this paper, we use the phenomenological kinetic model, which does not take into account the dynamic mechanism of the whole reaction process, only a simple formula to represent the interaction of the parameters in the reaction. For 3501-6 epoxy resin, the curing kinetics equation is [1, 2, 27]:

$$\begin{cases} \dfrac{d\alpha}{dt} = (K_1 + K_2\alpha)(1-\alpha)(0.47-\alpha) & \alpha \le 0.3 \\ \dfrac{d\alpha}{dt} = K_3(1-\alpha) & \alpha > 0.3 \end{cases} \tag{3}$$

where K_i $(i = 1, 2, 3)$ are the curing rate constants, and can be defined generally by the Arrhenius equations:

$$K_i = A_i \exp\left(\frac{-\Delta E_i}{RT}\right), \quad (i = 1, 2, 3) \tag{4}$$

Table 1 Thermo-physical properties of AS4 carbon fiber and 3501-6 epoxy resin [1, 2, 27]

Property	Value
Resin density ρ_r ($\mathrm{kg \cdot m^{-3}}$)	$90\alpha + 1232 (\alpha \le 0.45)$ 1272 $(\alpha \ge 0.45)$
Fiber density ρ_f ($\mathrm{kg \cdot m^{-3}}$)	1790
Resin specific heat capacity C_{pr} ($\mathrm{J \cdot kg^{-1} \cdot K^{-1}}$)	$4184[0.468 + 5.975 \times 10^{-4}T - 0.141\alpha]$
Fiber specific heat capacity C_{pf} ($\mathrm{J \cdot kg^{-1} \cdot K^{-1}}$)	$1390 + 4.50T$
Thermal conductivity of resin k_r ($\mathrm{W \cdot m^{-1} \cdot K^{-1}}$)	$0.04184[3.85 + (0.035T - 0.141)\alpha]$
Thermal conductivity of fiber k_f ($\mathrm{W \cdot m^{-1} \cdot K^{-1}}$)	$0.742 + 9.02 \times 10^{-4}T$

where R is the universal gas constant; ΔE_i are the activation energies, and A_i are the frequency factors obtained from experiments. The cure kinetic parameters of 3501-6 epoxy resin are shown in Table 2.

2.3 Elastic Model

Residual stress is usually caused by thermal expansion and chemical shrinkage. Thus, the stress-strain relation can be defined as [28]:

$$\{\sigma\} = [E](\{\varepsilon_{tot}\} - \{\varepsilon_{tc}\}) + \{\sigma_0\} \tag{5}$$

in which:

$$\{\varepsilon_{tc}\} = \{\varepsilon_{th}\} + \{\varepsilon_{ch}\} = \{\phi \Delta T\} + \{\varphi \Delta \alpha\} \tag{6}$$

where σ and σ_0 are the internal stress and initial stress, respectively; E is the elastic modulus; ε_{tot}, ε_{tc}, ε_{th}, and ε_{ch} are the total strain, free thermo-chemical strain, thermal expansion strain and chemical shrinkage strain, respectively, and free thermo-chemical strain is the superposition of the thermal strain and chemical shrinkage strain; ϕ and φ are the coefficient of thermal expansion (CTE) and chemical shrinkage (CCS) in each direction. The elastic modulus of resin can be expressed as:

$$E_m = \left(1 - \frac{\alpha - \alpha_{gel}}{1 - \alpha_{gel}}\right) E_m^0 + \frac{\alpha - \alpha_{gel}}{1 - \alpha_{gel}} E_m^\infty \tag{7}$$

where E_m^0 and E_m^∞ are the elastic modulus of uncured and completely cured resin; α_{gel} is the DOC at gel point of the resin.

2.4 Viscoelastic Model

In the curing process, the thermal expansion and chemical shrinkage of the composite laminates are liable to cause residual stresses. Using the time-cure-temperature superposition method and assuming that the laminates have no strain occurs before $t = 0$, the stress of the viscoelastic material can be determined by the following formula [23, 24, 29]:

$$\underline{\sigma}(t) = \int_0^t \underline{\underline{C}}(\alpha, T, t - \tau) \frac{d}{d\tau} \left[\underline{\varepsilon}_{tot}(\tau) - \underline{\varepsilon}_{tc}(\tau)\right] d\tau \tag{8}$$

in which:

$$\underline{\varepsilon}_{tc} = \underline{\varepsilon}_{th} + \underline{\varepsilon}_{ch} = \underline{\phi} \Delta T + \underline{\varphi} \Delta \alpha \tag{9}$$

where $\underline{\underline{C}}$ is the relaxation stiffness matrix as functions of DOC, temperature and time; t, τ, $\underline{\varepsilon}_{tot}$

Table 2 Cure kinetic parameters of 3501-6 epoxy resin [1, 2, 27]

Parameter	Value	Parameter	Value
A_1 (min^{-1})	2.102×10^9	ΔE_1 (J/mol)	8.07×10^4
A_2 (min^{-1})	-2.014×10^9	ΔE_2 (J/mol)	7.78×10^4
A_3 (min^{-1})	1.96×10^5	ΔE_3 (J/mol)	5.66×10^4
H_R (J/kg)	1.989×10^5	R ($\text{J} \cdot \text{mol}^{-1} \cdot \text{K}^{-1}$)	8.3143

and $\underline{\varepsilon}_{tc}$ are the current time, past time, total strain and free thermo-chemical strain, respectively. Free thermo-chemical strain includes thermal expansion strain, $\underline{\varepsilon}_{th}$, and cure shrinkage strain, $\underline{\varepsilon}_{ch}$. $\underline{\phi}$ and $\underline{\varphi}$ are the coefficient of thermal expansion (CTE) and shrinkage expansion (CSE) in each direction, respectively. In this paper, the double underlines and single underlines are respectively used to indicate the matrices and vectors. According to the characteristics of thermorheologically simple materials at a constant DOC, Eq. (8) can be rewritten as:

$$\underline{\sigma}(t) = \int_0^t \underline{\underline{C}}\left(\xi(t) - \xi'(\tau)\right) \frac{d}{d\tau}\left[\underline{\varepsilon}_{tot}(\tau) - \underline{\varepsilon}_{tc}(\tau)\right] d\tau \tag{10}$$

in which:

$$\xi(t) = \int_0^t \frac{dt'}{a_T\left[\alpha_{ref}, T(t')\right]}, \quad \xi(\tau) = \int_0^\tau \frac{dt'}{a_T\left[\alpha_{ref}, T(t')\right]} \tag{11}$$

where $\xi(t)$ and $\xi(\tau)$ are the current reduced time and past reduced time, respectively; α_{ref} is reference DOC, and a_T is the shift factor which allows for time-temperature superposition.

Based on the generalized Maxwell model with n Maxwell elements in parallel, the relaxation modulus of a viscoelastic material can be expressed by a Prony series as [30]:

$$E(\alpha, \xi) = E^{\infty}(\alpha) + \left[E^{u}(\alpha) - E^{\infty}(\alpha)\right] \sum_{i}^{n} W_i(\alpha) \exp\left[\frac{-\xi(\alpha, T)}{\tau_i(\varepsilon)}\right] \tag{12}$$

where E^{∞} and E^{u} are the fully relaxed and unrelaxed modulus. W_i is weigh factor. Based on the micro-mechanics theory [1], the proposed relaxation modulus and the unrelaxation materials properties, such as elastic modulus, shear modulus, Poisson's ratio, CTE and CSE, can be used to calculate the viscoelastic behavior of the anisotropic composites laminates accurately. The relaxation time and trade-off factors for AS4/3501-6 at reference curing degrees are shown in Table 3. Since the modulus in the fiber direction mainly reflects the performance of the fiber, and is constant, it is generally considered that E_{1N}^{u} is equal to E^{∞} for the fiber-reinforced material, so that the non-relaxation modulus of each Maxwell unit can be expressed as [2]:

Table 3 Relaxation times and weight factors at the reference degree of cure ($\alpha_r = 0.98$) [1]

m	τ_m(min)	W_m
1	2.922137e1	0.0591334
2	2.921437e3	0.0661255
3	1.82448e5	0.0826896
4	1.1031059e7	0.112314
5	2.8305395e8	0.154121
6	7.9432822e9	0.2618288
7	1.953424e11	0.1835594
8	3.3150756e12	0.0486939
9	4.9174856e14	0.0252258

Table 4 Elastic mechanical properties of AS4/3501–6 prepreg constituents [1, 2, 23]

Poperty	AS4 carbon fiber	3501-6 epoxy resin
Longitudinal elastic modulus E_1 (GPa)	206.8	3.2
Transverse elastic modulus $E_2 = E_3$ (GPa)	17.2	3.2
In-plane shear modulus $G_{12} = G_{13}$ (GPa)	27.58	1.185
Transverse shear modulus G_{23} (GPa)	6.894	1.185
In-plane Poisson's ratio $\upsilon_{12} = \upsilon_{13}$	0.2	0.35
Transverse Poisson's ratio υ_{23}	0.3	0.35
Longitudinal CTE ϕ_1 (1/˚C)	-9×10^{-7}	5.76×10^{-5}
Transverse CTE $\phi_2 = \phi_3$ (1/˚C)	7.2×10^{-6}	5.76×10^{-5}
Longitudinal CSE φ_1	0	−0.01695
Transverse CSE $\varphi_2 = \varphi_3$	0	−0.01695

$$
\begin{aligned}
&E_{1_i}^{u} = 0, (i = 1, N-1)\\
&E_{1_N}^{u} = E_1^{\infty} = E_1^{u}\\
&E_{2_i}^{u} = \left(E_2^{u} - E_2^{\infty}\right) W_i(\alpha), (i = 1, N-1)\\
&E_{2_N}^{u} = E_2^{\infty}\\
&G_{12_i}^{u} = \left(G_{12}^{u} - G_{12}^{\infty}\right) W_i(\alpha), (i = 1, N-1)\\
&G_{12_N}^{u} = G_{12}^{\infty}\\
&G_{23_i}^{u} = \left(G_{23}^{u} - G_{23}^{\infty}\right) W_i(\alpha), (i = 1, N-1)\\
&G_{23_N}^{u} = G_{23}^{\infty}
\end{aligned}
\tag{13}
$$

The unrelaxed mechanical properties (*i.e.* elastic mechanical properties) of AS4/3501-6 prepreg constituents are shown in Table 4. In addition, the mechanical properties of AS4/3501-6 prepreg can be calculated by micromechanical formulas (22)-(30) presented in Appendix.

3 Simulation Model Implementation

Based on the theoretical model proposed in the previous section, finite element analysis software (version 4.3b) of the COMSOL multi-physics coupling is used to simulate the curing process of the composite laminate. The simulation of curing process-induced residual stress and deformation for the composites is implemented by the linear elastic approach and the viscoelastic approach. The two sets of the results are compared with each other while White and Kim's research is also used as the reference [31, 32].

The two models respectively consist of three parts: a heat transfer module, a curing kinetic module and a mechanical (linear elastic or viscoelastic) module. There is a certain coupling between these modules. The two modules of heat conduction and curing kinetics are coupled to each other and are collectively referred to as thermochemical module. The calculation of these modules can be achieved by calling the corresponding application module in COMSOL software:

(1) Using the software 'heat transfer' application module to simulate the heat conduction model. In the module, enter the initial temperature of the material, the curing process parameters (boundary conditions) and the thermo physical performance parameters (see

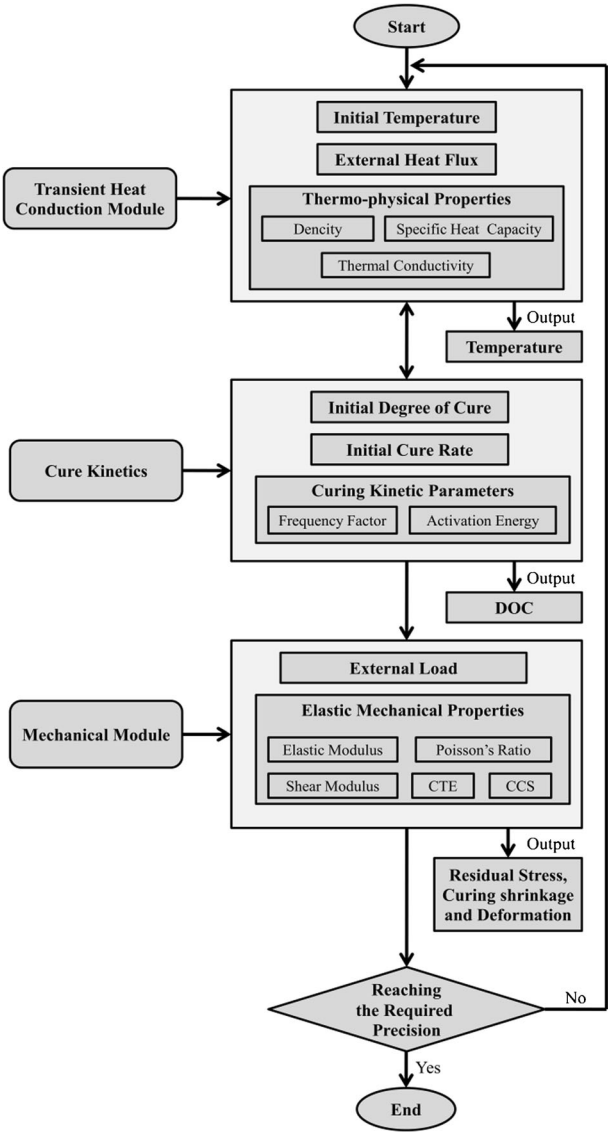

Fig. 1 Flow diagram of coupling calculation of curing process

Table 1). At the same time, the curing value obtained from the second module is called by calculating the three-dimensional transient heat conduction control Eq. (1), and then the temperature distribution of each node at the current time is obtained, which is the curing temperature field of the laminates.

(2) Using the 'coefficient type partial differential equation' application module in the software to simulate the curing dynamics model. The general form of the coefficient partial differential equation is:

$$f = e_a \frac{\partial^2 u}{\partial t^2} + d_a \frac{\partial u}{\partial t} + \nabla\cdot(-c\nabla u - \alpha u + \gamma) + \beta\cdot\nabla u + au \tag{14}$$

where u and t are the dependent variable and the transient time respectively; c, a, e_a, d_a, α, β and γ are the undetermined coefficients. f is the source term. By appropriately setting the coefficients and source terms, the formula (14) is transformed into the form of the curing kinetics Eq. (3). The initial curing degree and the curing kinetics parameter (see Table 2) are input and the calculation is performed by the heat transfer module. The temperature distribution of the composite skin is obtained by solving the Eq. (3).

(3) Simulating the mechanical model by using the 'Structural Mechanics' application module. In this item, entering the boundary load, relaxation factor, relaxation time (see Table 3) and elastic mechanical performance parameters (see Table 4), and calling the 'heat transfer' module and the 'coefficient type partial differential equation' module. The residual stress distribution, curing shrinkage and curing deformation of the laminates are obtained by solving the strain Eqs. (8) and (9).

Figure 1 is a flow diagram of coupling calculation of curing process. The new state parameters calculated in the above process are resin density, specific heat capacity, thermal conductivity, thermal expansion coefficient and modulus, etc.. It needs to update these state parameters in the next analysis step to solve the coupling.

4 Material Model Verification

A same-thickness-plies orthotropic composite laminate with a stacking sequence of [0° / 90° / 90° / 0°] is taken as an example, as shown in Fig. 2. Its size is about $10.16cm \times 10.16cm \times 2.54cm$. Through the effective grid verification, a hexahedral mesh is employed as refined

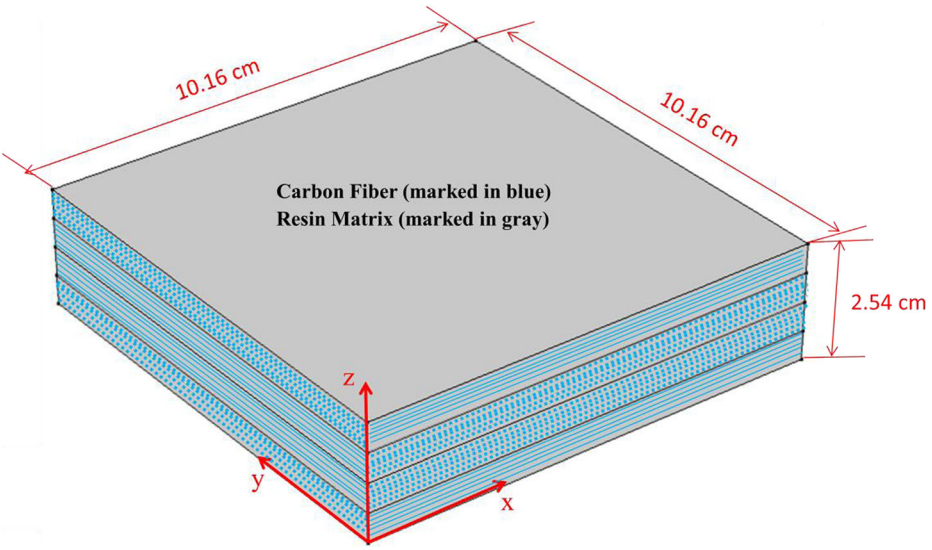

Fig. 2 Schematic of the composite laminates

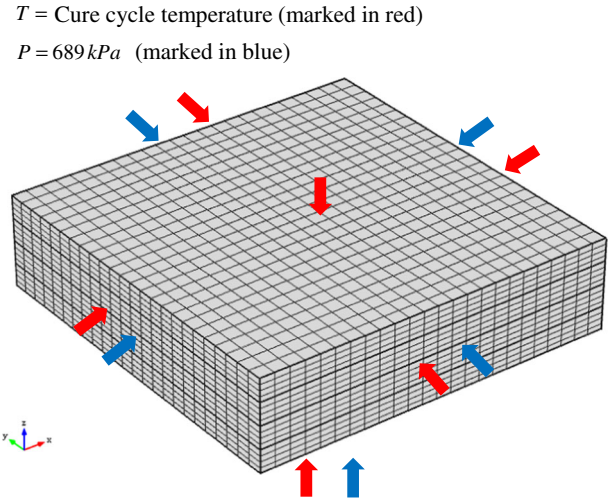

Fig. 3 Boundary conditions and meshing of the composite laminates

mesh (see in Fig. 3). The number of elements for per layer is 2304, and the total number is 9216. AS4/3501-6 prepreg containing AS4 fibers preimpregnated with 3501-6 epoxy resin is used as the primary material, and the performance parameters of 350-6 epoxy resin and AS4 carbon fiber material are shown in Tables 1 and 4.

Cure cycle recommended from the manufacturer (the short dash line shown in Fig. 4) is used in these simulations. It consists of five stages: the first heating stage in which the temperature is increased from 25 °C to 116 °C at the rate of, after 1 h of incubation and then enters the second holding stage with the same ramp rate to 177°C, and finally, cool-down cycle with a ramp rate of −2.5 °C / min from 177 °C to 25 °C. Two boundary conditions are set at the interface between the mold and the component: heat and pressure. As shown in Fig. 3, the curing process parameters of the mold heating are provided on the outer surface of the laminate, and a pressure load of 689 kPa is applied to the side and bottom surfaces.

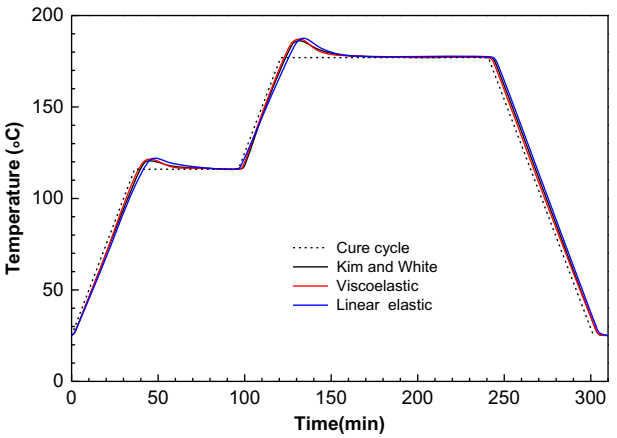

Fig. 4 Development of temperature in central point (5.08, 5.08, 1.27) of the composite laminate under manufacture recommended cure cycle

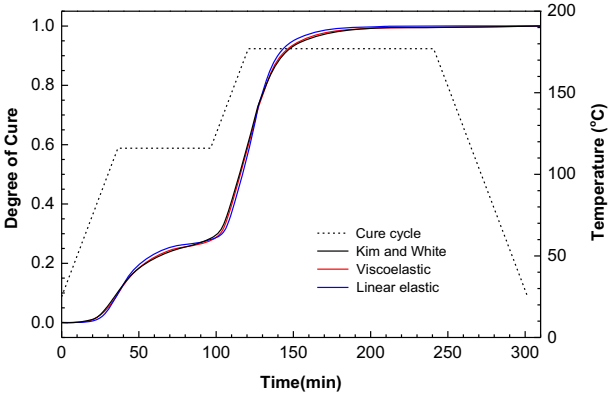

Fig. 5 Development of DOC in central point (5.08, 5.08, 1.27) of the composite laminate under manufacture recommended cure cycle

5 Results and Discussion

5.1 Thermo-chemical Analysis

Figures 4 and 5 show the comparison of the temperature and DOC in central point (5.08, 5.08, 1.27) for the laminate between the linear elastic model and the viscoelastic model respectively under manufacture recommended cure cycle. The other result presented by Kim and White [31] are also displayed. Figure 6 is the development of temperature on a line from surface point (5.08, 5.08, 0) to central point (5.08, 5.08, 1.27) of the composite laminate. It can be seen from these figures that the calculated results of the two models are very close to those in literature. In the first heating stage, since the external first heat, and the internal resin has not yet violent reaction, so the center temperature is lower than the ambient temperature. In the next incubation stage, the center temperature rises rapidly and reaches the first peak 122 °C at 45 min., while the cross linking rate accelerates as the result of heat conduction and reaction heat accumulation. In the second warming stage, the center temperature is again lower than the ambient temperature due to the lower thermal

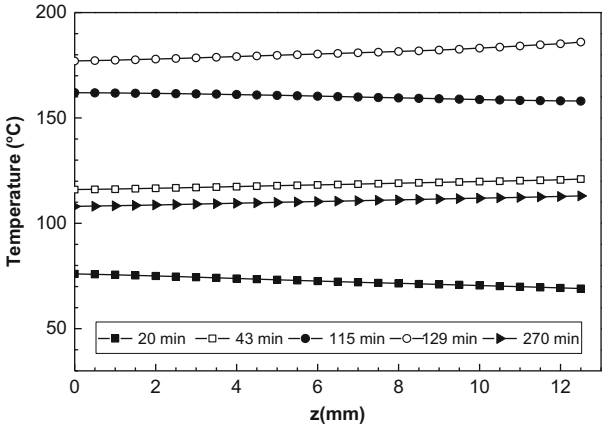

Fig. 6 Development of temperature on a line from surface point (5.08, 5.08, 0) to central point (5.08, 5.08, 1.27) of the composite laminate

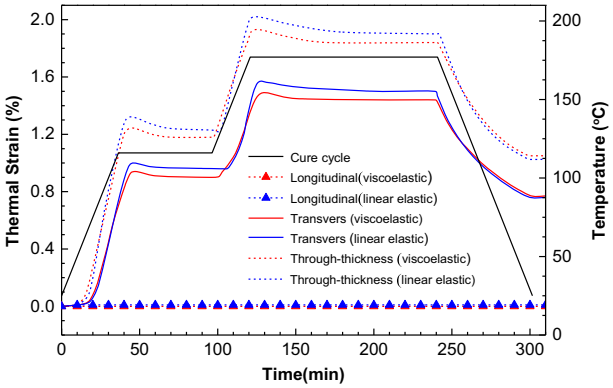

Fig. 7 Comparison of thermal strain in different directions at the point (5.08, 0, 1.27) from the linear elastic and viscoelastic models

conductivity and thermal conductivity of the composite, but the cross-linking reaction is more intense. After entering the second incubation stage, the high temperature region is transferred to the inside again with the heat transfer and the internal heat release, and reaches the second peak at 187 °C at 131 min. Finally, during the cooling phase, as the curing reaction is substantially complete, the heat release is reduced and the center temperature gradually approaches room temperature. The results indicate that both the heat conduction and cure kinetics modules are quite qualified to simulate thermo-chemical response for the composite laminate during cure cycle.

5.2 Residual Stress Analysis

In this section, the development of process-induced residual stress is analyzed. The cure shrinkage is the major factor leading to residual stress generation, and it is composed of the chemical shrinkage and thermal strains. Figure 7 shows the altered state of thermal strain in different directions at the points 5.08, 0 and 1.27 for the composite laminate during cure cycle. Thermal strain in the longitudinal direction is negligible, and those in through-thickness and transverse directions change obviously, especially during two heating stages. But the difference between the linear elastic model and the viscoelastic model is great during heating and holding stages since the former doesn't consider the relaxation properties of materials. Figure 8 shows Comparison of cure

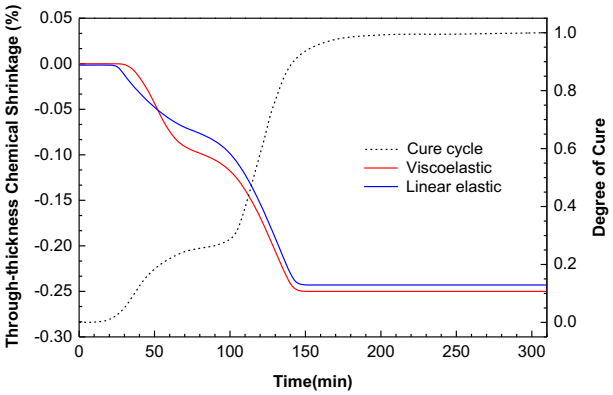

Fig. 8 Comparison of cure shrinkage in the through-thickness direction from the linear elastic and viscoelastic models

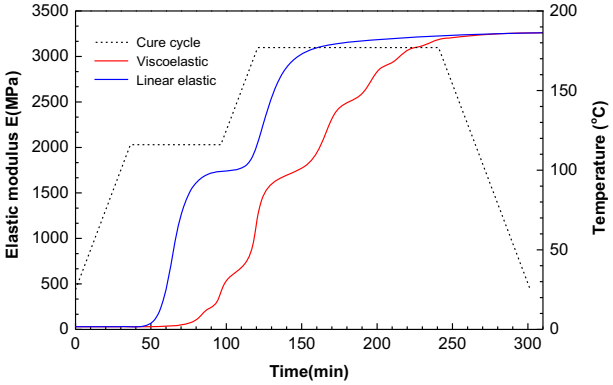

Fig. 9 Comparison of elastic modulus in through-thickness direction during cure cycle from the linear elastic and viscoelastic models at constant frequency 0.1 Hz

shrinkage in the through-thickness direction from these two models. The same to the contrast result of thermal strain, the chemical shrinkage of the two models is very different from the simulated DOC during cure cycle. Because of the lateral pressure, the chemical shrinkage in x and y directions are negligible while the one in the through-thickness direction is obvious.

Figures 9 and 10 show the simulated results of elastic modulus in through-thickness direction and shear modulus development calculated respectively by the linear elastic model and the viscoelastic model during cure cycle. Obviously, both the elastic and shear modulus calculated by the viscoelastic approach increases slowly during curing and continues growing during cool-down stage. Moreover, there is a great difference between the two models.

Figures 11 and 12 show the development of interlaminar normal stress σ_3 at the points 5.08, 0, 1.27 and transverse stress σ_2 in the 0° ply at $x = 5.08$ and $y = 5.08$ of the laminate. It can be seen that the results of the viscoelastic model are well consistent with that presented by White and Kim [32]. Figure 11 shows that the final stress for the normal stress from the linear elastic model is 28.2 MPa, which is 20% greater than the viscoelastic solution, while the final stress for the transverse stress from the linear elastic model in Fig.

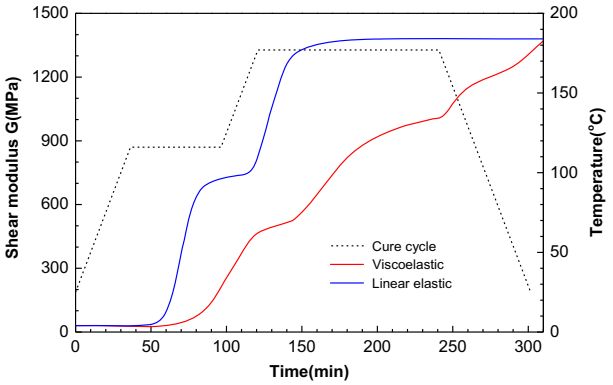

Fig. 10 Comparison of shear modulus during cure cycle from the linear elastic and viscoelastic models at constant frequency 0.1 Hz

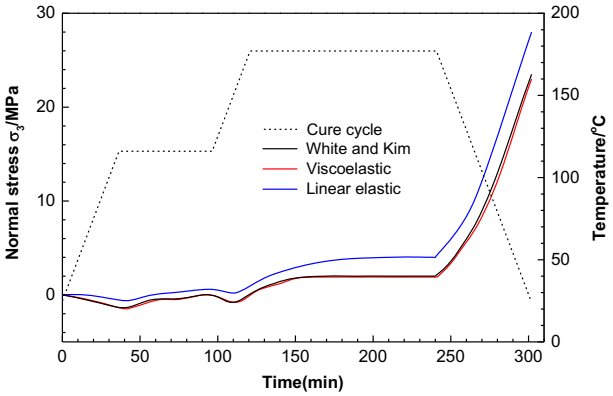

Fig. 11 Development of interlaminar normal stress σ_3 at the point (5.08, 0, 1.27) of the composite laminate under manufacture recommended cure cycle

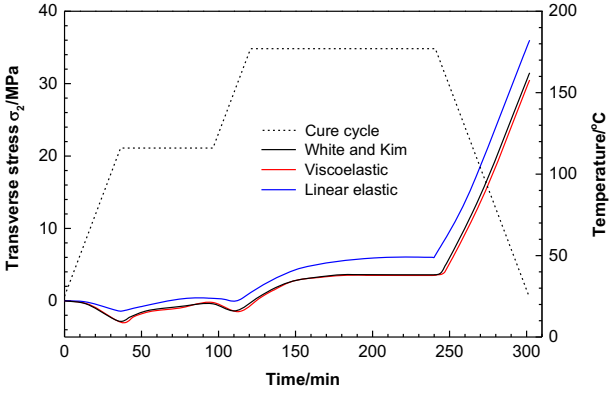

Fig. 12 Development of transverse stress σ_2 in the 0° ply at $x = 5.08$ and $y = 5.08$ of the composite laminate under manufacture recommended cure cycle

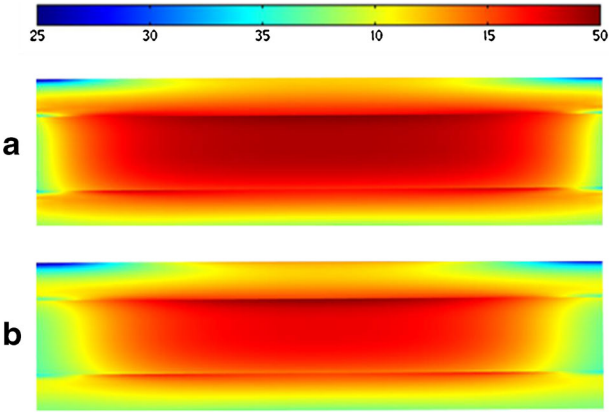

Fig. 13 Contours of Von Minses stresses on the cross section y = 5.08 at the end of cure cycle from the two models. **a** Linear elastic model, **b** Viscoelastic model

12 is 35.9 MPa, which is 14% greater than the viscoelastic solution. Figure 13 illustrates the von Minses stress distribution of the composite laminate on the cross section y = 5.08 after cool-down predicted by the linear elastic model and the viscoelastic model respectively.

5.3 Curing Deformation Analysis

Maximum deformation defined as the maximum absolute displacement in the through-thickness direction is introduced to indicate the gap of the deformation between the viscoelastic and modified CHILE models. Figure 14 shows the curing deformation contour predicted by the linear elastic model and the viscoelastic model after cool-down. It is evident that the laminate curves identically from four corners due to the symmetrical and uniform laying of the fibers. And the degree of deformation predicted by the linear elastic model is larger than the viscoelastic model's. The maximum deformation estimated by the linear elastic model is 0.81 cm, which is 0.08 cm larger than the viscoelastic model's (0.73 cm).

Besides prediction accuracy, a significant difference of computation time is also observed between the two models. In heating and holding stages, the linear elastic model approximately runs 14 times faster than the viscoelastic model.

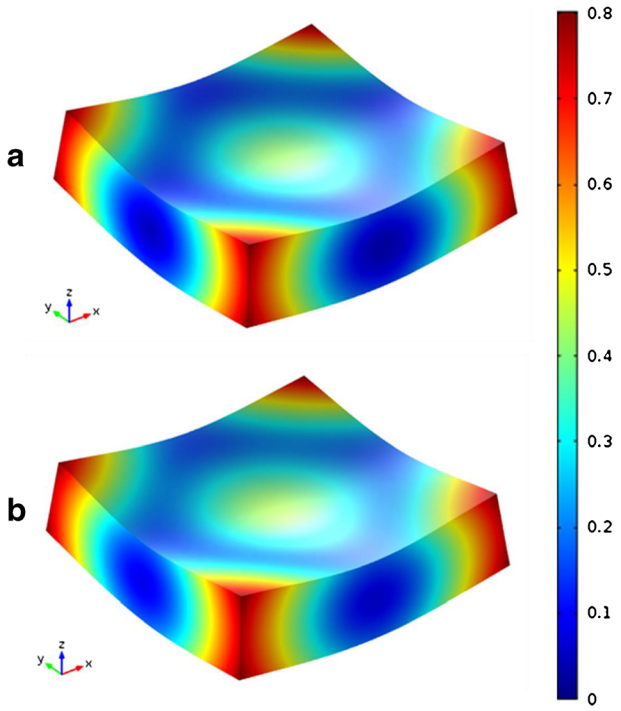

Fig. 14 Contours of the deformation after cool-down predicted by the two models. **a** Linear elastic model, **b** Viscoelastic model

6 Conclusions

In this paper, the three-dimensional transient multi-physics coupling finite element analysis method has been used to simulate the curing process of the composites. Both the linear elastic model and viscoelastic model have been presented to predict temperature, DOC, process-induced residual stress and deformation for the thermosetting resin composite laminates. The coupling relationship between the physical and chemical changes has been taken into account.

A four-layer composite laminate has been established to validate the two simulation models. The results showed that the curing temperature, DOC, cure shrinkage and residual stress predicted by the viscoelastic model are in good agreement with those obtained by Kim and White, but in the linear elastic model, there are only temperature and DOC to be consistent with results of literature. In addition, the maximum deformation obtained from the linear elastic model is obviously larger than that calculated by the viscoelastic model within acceptable limits.

Moreover, the linear elastic model could replace the viscoelastic model within the margin of error for a much more efficient numerical implementation and shorter computation time. It suggested that these two models proposed in this paper have strong applicability, and have certain guiding significance to improve the curing process parameters and control the curing deformation of the skin surface parts.

Acknowledgements The author would like to thank "Jing Hou Xin" research group for many fruitful discussions. This work is supported by the National Natural Science Foundation of China (Grant No. 11664023).

Appendix

This appendix presents micromechanical homogenization equations which used to determine the overall composite properties of unidirectional lamina. Noted that subscripts f and r represent fiber and resin, respectively. The thermo-physical properties of the composites, including the density, ρ, the specific heat capacity, C_p, and the longitudinal thermal conductivity, k_L, (x -direction in Eq. (1)), can be respectively calculated by the following rule of mixtures [33]:

$$\rho = v_f \rho_f + \left(1-v_f\right)\rho_r \tag{15}$$

$$C_p = \frac{\rho_f v_f C_{pf} + \rho_r \left(1-v_f\right) C_{pr}}{\rho} \tag{16}$$

$$k_L = v_f k_f + \left(1-v_f\right) k_r \tag{17}$$

The transverse thermal conductivity of the composites, k_T, (y and z -direction in Eq. (1)) can be calculated based on the E-S model [34]. It is given as:

$$\frac{k_T}{k_r} = \left(1-2\sqrt{v_f \Big/ \pi}\right) + \frac{1}{2B}\left[\pi - \left(4 \Big/ \sqrt{1-\beta}\right)\tan^{-1}\left(\sqrt{1-\beta} \Big/ 1+\beta\right)\right] \tag{18}$$

in which:

$$\beta = B^2 v_f \Big/ \pi \tag{19}$$

$$B = \mu\left(k_r \Big/ k_f - 1\right) \tag{20}$$

$$\mu = a \Big/ b \tag{21}$$

where a and b are the axial lengths of the elliptic section of the fiber along the y -axis and z -axis, respectively. In this paper, the cross section of the fiber is round, so a is equal to b, *i.e.* $\mu = 1$.

Self-consistent micromechanics homogenization equations [32] used to determine the composite properties are listed in this appendix. Subscripts 1, 2 and 3 represent the principal directions of unidirectional lamina. The Young's modulus of the composites in the longitudinal direction of the fiber is expressed as:

$$E_1 = E_{1f} v_f + E_r\left(1 - v_f\right) + \frac{4\left(\upsilon_r - \upsilon_{12f}\right)^2 K_r K_f G_r v_f \left(1 - v_f\right)}{\left(K_f + G_r\right) K_r + \left(K_f - K_r\right) G_r v_f} \tag{22}$$

in which:

$$K_f = \frac{E_{1f} E_{2f}}{2\left(1 - \upsilon_{23f}\right) E_{1f} - 4\upsilon_{12f}^2 E_{2f}} \tag{23}$$

$$K_r = \frac{E_r}{2(1 - \upsilon_r) - 4\upsilon_r^2} \tag{24}$$

where E_{1f} and E_{2f} are the Young's modulus of the fiber in the longitudinal direction and transverse direction; E_r is the Young's modulus of the resin; G_r is the shear modulus of the resin; υ_{12f} and υ_{23f} are the in-plane Poisson's ratio and transverse Poisson's ratio of the fiber; υ_r is the Poisson's ratio of the resin; K_f and K_r are the bulk modulus of the fiber and resin, respectively.

The in-plane shear modulus of the composites is expressed as:

$$G_{12} = G_{13} = G_r \frac{\left(G_{12f} + G_r\right) + \left(G_{12f} - G_r\right) v_f}{\left(G_{12f} + G_r\right) - \left(G_{12f} - G_r\right) v_f} \tag{25}$$

The out-of-plane shear modulus of the composites is expressed as:

$$G_{23} = G_r \frac{\left(G_{23f} + G_r\right) K_r + 2G_{23f} G_r + \left(G_{23f} - G_r\right) K_r v_f}{\left(G_{23f} + G_r\right) K_r + 2G_{23f} G_r - \left(G_{23f} - G_r\right)\left(K_r + 2G_r\right) v_f} \tag{26}$$

where G_{12f} and G_{23f} are the in-plane shear modulus and out-of-plane shear modulus of the fiber, respectively.

The plane strain bulk modulus of the composites is expressed as:

$$K_2 = \frac{(K_f + G_r)K_r - (K_f - K_r)G_r v_f}{(K_f + G_r) - (K_f - K_r)v_f} \tag{27}$$

The Young's modulus of the composites in the transverse direction of the fiber is expressed as:

$$E_2 = E_3 = \frac{1}{1/4K_2 + 1/4G_{23} + \upsilon_{12}^2/E_1} \tag{28}$$

The in-plane Poisson's ratio of the composites is expressed as:

$$\upsilon_{12} = \upsilon_{13} = \upsilon_{12f} v_f + \upsilon_r(1 - v_f) + \frac{(\upsilon_r - \upsilon_{12f})(K_r - K_f)G_r v_f v_r}{(K_f + G_r)K_r + (K_f - K_r)G_r v_f} \tag{29}$$

The out-of-plane Poisson's ratio of the composites is expressed as:

$$\upsilon_{23} = 1 - \frac{E_1 E_2 + 4\upsilon_{12}^2 E_2 K_2}{2E_1 K_2} \tag{30}$$

The longitudinal CTE of the composites is expressed as:

$$\phi_1 = \frac{v_f \phi_{1f} E_{1f} + (1 - v_f)\phi_m E_{1m}}{v_f E_{1f} + (1 - v_f)E_{1m}} \tag{31}$$

The transverse CTE of the composites is expressed as:

$$\begin{aligned} \phi_2 = \phi_3 = {} & v_f(\phi_{2f} + \upsilon_{12f}\phi_{1f}) + v_m(1 + \upsilon_m)\phi_m \\ & - (\upsilon_{12f} v_f + \upsilon_m v_m)\frac{\phi_{1f} E_{1f} v_f + \phi_{1m} E_{1m} v_m}{E_{1f} v_f + E_{1m} v_m} \end{aligned} \tag{32}$$

References

1. Bogetti, T.A., Gillespie, J.W.: Process-induced stress and deformation in thick-section thermoset composite laminates. J. Compos. Mater. 26(5), 626–660 (1992)
2. Griffin, O.H.: Three-dimensional curing stresses in symmetric cross-ply laminates with temperature-dependent properties. J. Compos. Mater. 17(5), 449–463 (1983)
3. Hahn, H.T.: Residual stresses in polymer matrix composite laminates. J. Compos. Mater. 10(4), 266–277 (1976)
4. Costa, V., Sousa, A.: Modeling of flow and thermo-kinetics during the cure of thick laminated composites. Int. J. Therm. Sci. 42(1), 15–22 (2003)
5. Shin, D.D., Hahn, H.T.: Compaction of thick composites: simulation and experiment. Polym. Compos. 25(1), 49–59 (2004)
6. Svanberg, J.M., Holmberg, J.A.: Prediction of the shape distortions part I: FE implementation of a path dependent constitutive model. Compos A: Appl Sci Manuf. 35(6), 711–721 (2004)
7. Adolf, D.B., Chambers, R.S.: A thermodynamically consistent, nonlinear viscoelastic approach for modelling thermosets during cure. J. Rheol. 51(1), 23–50 (2007)
8. Ganapathi, A.S., Joshi, S.C., Chen, Z.: Simulation of Bleeder flow and curing of thick composites with pressure and temperature dependent properties. Simul Model Pract Theory. 32(1), 64–82 (2013)
9. Abdelal, G.F., Robotham, A., Cantwell, W.: Autoclave cure simulation of composites structures applying implicit and explicit FE techniques. Int. J. Mech. Mater. Des. X9x(1), 55–63 (2013)

10. Vautard, F., Ozcan, S., Poland, L.: Influence of thermal history on the mechanical properties of carbon fiber-acrylate composites cured by electron beam and thermal processes. Compos A: Appl Sci Manuf. X45X(2), 162–172 (2013)
11. Curiel, T., Fernlund, G.: Deformation and stress build-up in bi-material beam specimens with a curing FM 300 adhesive interlayer. Compos A: Appl Sci Manuf. 39(2), 252–261 (2008)
12. Wisnom, M.R., Gigliotti, M., Ersoy, N., Campbell, M., Potter, K.D.: Mechanisms generating residual stresses and distortion during manufacture of polymer-matrix composite structures. Compos A: Appl Sci Manuf. X37(4), 522–529 (2006)
13. Ruiz, E., Trochu, F.: Numerical analysis of cure temperature and internal residual stresses in thin and thick RTM parts. Compos A: Appl Sci Manuf. 36x(6), 806–826 (2005)
14. Jansen, K.M.B., De Vreugd, J., Ernst, L.J.: Analytical estimate for curing-induced stress and warpage in coating layers. J. Appl. Polym. Sci. 126(5), 1623–1630 (2012)
15. Tavakol, B., Roozbehjavan, P., Ahmed, A., Das, R., Joven, R., Koushyar, H.: Prediction of residual stresses and distortion in carbon fiber-epoxy composite parts due to curing process using finite element. J. Appl. Polym. Sci. 128(2), 941–950 (2013)
16. White, S.R., Hahn, H.T.: Process modeling of composite materials: residual stress development during cure. Part II. Experimental validation. J. Compos. Mater. 26(16), 2423–2453 (1992)
17. Prasatya, R., McKenna, G.B., Simon, S.L.: A viscoelastic model for predicting isotropic residual stresses in thermosetting materials: effects of processing parameters. J. Compos. Mater. 35(10), 826–849 (2001)
18. Khoun, L., Hubert, P.: Investigation of the dimensional stability of carbon epoxy cylinders manufactured by resin transfer moulding. Compos A: Appl Sci Manuf. 41(1), 116–124 (2013)
19. Toudeshky, H.H., Sadighi, M., Vojdani, A.: Effects of curing thermal residual stresses on fatigue crack propagation of aluminum plates repaired by FML patches. Compos. Struct. 100(6), 154–162 (2013)
20. Wang, X.X., Zhao, Y.R., Su, H., Jia, Y.X.: Curing process-induced internal stress and deformation of fiber reinforced resin matrix composites: numerical comparison between elastic and viscoelastic models. Polym. Polym. Compos. 24(2), 155–160 (2016)
21. Stango, R.J., Wang, S.S.: Process-induced residual thermal stresses in advanced fiber-reinforced composite laminates. J. Manuf. Sci. Eng. 106(1), 48–54 (1984)
22. Shokrieh, M.M., Kamali, S.M.: Theoretical and experimental studies on residual stresses in laminated polymer composites. J. Compos. Mater. 39(24), 2213–2225 (2005)
23. KimYK, W.S.R.: Stress relaxation behavior of 3501-6 epoxy resin during cure. Polym. Eng. Sci. 36(23), 2852–2862 (1996)
24. O'Brien, D.J., Mather, P.T., White, S.R.: Viscoelastic properties of an epoxy resin during cure. J. Compos. Mater. 35(10), 883–904 (2001)
25. Patham, B.: Multiphysics simulations of cure residual stresses and springback in a thermoset resin using a viscoelastic model with cure-temperature-time superposition. J. Appl. Polym. Sci. 129(3), 983–998 (2013)
26. Taylor, R.L., Pister, K.S., Goudreau, G.L.: Thermo-mechanical analysis of viscoelastic solids. Int. J. Numer. Methods Eng. 2(1), 45–59 (1970)
27. Kim, Y.K., White, S.R.: Process-Induced stress relaxation analysis of AS4/3501-6 laminate. J. Reinf. Plast. Compos. 26(1), 2–16 (1997)
28. Hong, L.C., Hwang, S.J.: Study of warpage due to P-V-T-C relation of EMC in IC packaging. IEEE Trans Compon Packag Technol. 27, 291–295 (2004)
29. Salla, J.M., Ramis, X.: Comparative study of the cure kinetics of an unsaturated polyester resin using different procedures. Polym. Eng. Sci. 36(6), 835–850 (1996)
30. Johnston, A., Vaziri, R., Poursartip, A.: A plane strain model for process-induced deformation of laminated composite structures. J. Compos. Mater. 35(16), 1435–1469 (2001)
31. Kim, Y.K., White, S.R.: Viscoelastic analysis of processing-induced residual stresses in thick composite laminates. Mech. Compos. Mater. Struct. 4(4), 361–387 (1997)
32. White, S.R., Kim, Y.K.: Process-induced residual stress analysis of AS4/3501-6 composite material. Mech Compos Mater Struct. 5(2), 153–186 (1998)
33. Ma, Y.R., He, J.L., Li, D., Tan, Y., Xu, L.: Numerical simulation of curing deformation of resin matrix composite curved structure. Acta Materiae Compositae Sinica. 32(3), 874–880 (2015)
34. Tavman, I., Akinci, H.: Transverse thermal conductivity of fiber reinforced polymer composites. Int Commun Heat Mass. 27(2), 253–261 (2000)